Ocean Engineering 154 (2018) 226–233

Contents lists available at ScienceDirect

Ocean Engineering

journal homepage: www.elsevier.com/locate/oceaneng

Kadomtsev-Petviashvili type equation for uneven water depths

Serdar Beji

Faculty of Naval Architecture and Ocean Engineering, Istanbul Technical University, Maslak 34469, Istanbul, Turkey

ARTICLE INFO

Keywords:
Kadomtsev-petviashvili equation
Kortweg & de vries equation
Improved dispersion
Improved shoaling
Nonlinearity
Uneven water depths

ABSTRACT

A Kadomtsev-Petviashvili type equation with improved dispersion characteristics is derived for varying water depths. Linear shoaling characteristics of the equation for unidirectional waves are in accord with the principle of energy flux concept. A finite-difference scheme is devised to demonstrate the extended range of applications of the newly derived equation for a number of well-known cases. In addition, a permanent wave form with singularity is shown to be an exact solution of the KdV or unidirectional KP equations. The same form for an arbitrary direction satisfies the combined Boussinesq equations of any type.

1. Introduction

Kadomtsev and Petviashvili (1970) derived a directional version of Korteweg and de Vries (1895) equation to study the stability of solitary waves. Since then the Kadomtsev-Petviashvili equation or briefly the KP equation has found widespread application areas, and its various forms have been derived in the context of water waves. Bryant (1982) studied obliquely intersecting permanent waves by deriving a set of nonlinear equations which could describe fully-dispersive waves as well as weakly dispersive waves of the KP type, depending on the choice of the coefficients. Hammack et al. (1989) generated finite-amplitude two-dimensional shallow water waves in laboratory and mathematically described them by the exact solutions of the KP equation. Accurate representation of waves outside the validity range of the KP equation was indicated as a striking feature. Based on a Crank-Nicolson type formulation Feng and Mitsui (1998) proposed an implicit finite-difference scheme for numerical solutions of the original KdV and KP equations. In the same vein, Mekki and Ali (2013) employed a Cranck-Nicolson discretization for the solution of a KP equation derived from the so-called BBM equation of Benjamin et al. (1972). Modeling of dust-acoustic solitary wave in dusty plasmas by Xue (2003) may also be mentioned as a rather unusual application of the KdV or KP equation.

The origin of the KP equation, like that of the KdV equation, may be traced back to the work of Boussinesq (1872). The KdV equation is one-dimensional Boussinesq equation transformed to propagate unidirectional waves while the KP equation is directional form of the KdV equation. The present work derives a KP type equation with relatively better dispersion characteristics, based on a previous KdV type equation for varying depths (Beji, 2016). The improved dispersion properties enable the new equation to propagate shorter waves quite accurately in comparison with the existing KP models, which are basically restricted to long waves. Further, the newly derived linear shoaling terms of the present equation ensure that for unidirectional waves the shoaling rate is in perfect accord with the energy flux concept.

Numerical treatment of the new KP equation is done by a Crank-Nicolson type finite-difference formulation similar to Feng and Mitsui (1998). Numerous test cases are carried out, starting with examination of shoaling properties of the equation for varying bathymetry and continuing with simulations of truly two-dimensional obliquely intersecting cnoidal waves as in the experiments of Hammack et al. (1989). Then, nonlinear refraction-diffraction of waves over a converging zone as experimentally measured by Whalin (1971) are simulated. Finally, a rather difficult case of wave propagation over obliquely shoaling bottom topography with an obliquely situated elliptic shoal given by Berkhoff et al. (1982) is considered for comparisons with experimental results. All these simulations show clearly that the KP type equation derived here is capable of simulating shoaling, refraction and diffraction of relatively shorter linear and nonlinear waves with acceptable accuracy. As rightly noticed by Hammack et al. (1989), the capabilities of the KP equation are not strictly restricted to weakly directional waves. The extend of directionality encompassed by the KP equation is quite good but only slightly hindered by its linear non-dispersive character in transverse direction.

Finally, a peculiar permanent wave form analytically satisfying KdV or unidirectional KP equation of any type as well as the combined form of Boussinesq equations is obtained. The solution, being singular, is deemed of secondary importance from the physical point of view hence placed in the appendix.

E-mail address: sbeji@itu.edu.tr.

https://doi.org/10.1016/j.oceaneng.2018.01.054
Received 14 March 2017; Received in revised form 9 January 2018; Accepted 10 January 2018

2. KP type equation for uneven water depths

Before proceeding to the derivation of the improved KP equation, the derivation of a non-dispersive linear KP equation is considered briefly as a preliminary to the general case.

2.1. KP type equation based on linear long wave model

In order to outline the derivation procedure for the simplest case possible and at the same time to point out an interesting connection with the radiation boundary condition of Engquist and Majda (1977), first a KP-like equation is derived from the linear long wave equations. For constant depth the linearized shallow water equations are given by (Dingemans, 1997)

$$\eta_t + h\nabla\cdot\mathbf{u} = 0 \tag{1}$$

$$\mathrm{u}_t + g\nabla\eta = 0 \tag{2}$$

where $\mathbf{u}$ is the vertically averaged or mean horizontal velocity vector with components (u, v) and η is the free surface displacement as measured from the still water level. h is the water depth and g is the gravitational acceleration. ∇ stands for two-dimensional horizontal gradient operator with components $(\partial/\partial x, \partial/\partial y)$ while subscript t denotes partial differentiation with respect to time. By cross differentiations the above equations may be combined into a single equation in terms of η

$$\eta_{tt} - C^2\left(\eta_{xx} + \eta_{yy}\right) = 0 \tag{3}$$

in which $C = \sqrt{gh}$ is defined as the non-dispersive phase celerity. A co-ordinate system moving in the positive $x-$direction with the celerity C is now introduced so that wave form evolutions in this moving system are slow. New spatial $\sigma = x - Ct$ and temporal $\tau = \varepsilon t$ co-ordinates are employed with the small parameter ε indicating the weak changes of wave form in time in the moving co-ordinate system. No approximation has been introduced for the $y-$direction. However, the new co-ordinate system moves at the celerity C only in the $x-$direction, which is the preferred direction of the propagation; while directional waves would have a propagation velocity vector not necessarily in the $x-$direction. Thus, favoring a certain direction in (σ, τ) transformation would result in an unsymmetric wave equation. That is to say, unlike equation (3), the transformed equation would not be the same when x and y are interchanged. Expressing the terms in equation (3) in the new co-ordinate system gives

$$\eta_{tt} = C^2\eta_{\sigma\sigma} - 2C\varepsilon\eta_{\sigma\tau},\ \eta_{xx} = \eta_{\sigma\sigma} \tag{4}$$

where the term $O(\varepsilon^2)$ has been dropped as being higher-order than intended to keep. Substituting the above expressions for the relevant terms in equation (3) while keeping the $y-$direction term intact results in

$$-2C\varepsilon\eta_{\sigma\tau} - C^2\eta_{yy} = 0 \tag{5}$$

Going back to the original co-ordinate system requires the inverse transformation $\varepsilon\eta_{\sigma\tau} = \eta_{xt} + C\eta_{xx}$, which is substituted into equation (5) and the entire equation is divided by $-2C$ to obtain

$$\eta_{xt} + C\eta_{xx} + \frac{1}{2}C\eta_{yy} = 0 \tag{6}$$

which may be viewed as the linearized shallow water version of the KP equation. Solving equation (3) for η_{xx} and using it in equation (6) renders the second-order radiation boundary condition $\eta_{tt} + C\eta_{xt} - \frac{1}{2}C^2\eta_{yy} = 0$ (in dimensional form for right-going waves) derived by Engquist and Majda (1977) for directional waves. In this respect equation (6) suggests itself as a suitable boundary condition: it has no missing terms compared to equation (3) but supports only those waves moving in the positive $x-$direction. In other words, while only right-going waves are permitted left-going waves are not allowed and at the same time directional radiation of waves has not been compromised.

2.2. KP type equation based on improved Boussinesq model

Beji and Nadaoka (1996) introduced the concept of partial replacement of dispersion terms to the Boussinesq model of Peregrine (1967) for varying water depths. Their improved model, comprising continuity and momentum equations, may be combined into a single nonlinear wave equation in terms of the surface displacement η by suitable approximations to obtain

$$\begin{aligned}\eta_{tt} &= gh\nabla^2\eta - \frac{\beta}{3}gh^3\nabla^2\left(\nabla^2\eta\right) + \frac{(1+\beta)}{3}h^2\nabla^2\eta_{tt} + \frac{3}{2}g\nabla^2\left(\eta^2\right)\\ &+g\nabla h\cdot\nabla\eta - 2\beta gh^2\nabla h\cdot\nabla\left(\nabla^2\eta\right) + (1+\beta)h\nabla h\cdot\nabla\eta_{tt}\end{aligned} \tag{7}$$

in which only the terms containing the first spatial derivative of the depth are retained. Truncation of higher depth gradients corresponds to the *mild-slope* assumption, which is used throughout the present work wherever necessary. The coefficient β is a non-dimensional scalar controlling the dispersion characteristics of the equation. While $\beta = -1$ for 1-D results in the original derivation of Boussinesq (1872), $\beta = 0$ corresponds to the combined form of Peregrine's (1967) equations. Setting $\beta = 1/5$ results in an improved dispersion relationship which is in accord with the fourth-order Padé approximation of the linear theory dispersion relation.

In order to derive a KP type equation from equation (7) the $x-$direction is taken as the main propagation direction with all the relevant terms while only non-dispersive propagation in the $y-$direction is retained as in equation (3). All the other $y-$dependent terms; namely, the nonlinear, dispersive, and shoaling terms in the $y-$direction, are dropped. Such a truncation renders the propagation in the $y-$direction linear and non-dispersive and results in

$$\begin{aligned}\eta_{tt} &= gh\left(\eta_{xx} + \eta_{yy}\right) - \frac{\beta}{3}gh^3\eta_{xxxx} + \frac{(1+\beta)}{3}h^2\eta_{xxtt} + \frac{3}{2}g\left(\eta^2\right)_{xx}\\ &+gh_x\eta_x - 2\beta gh^2h_x\eta_{xxx} + (1+\beta)hh_x\eta_{xtt}\end{aligned} \tag{8}$$

With the exception of η_{yy} term the derivation procedure of the KP type equation from equation (8) is completely identical with the derivation of the KdV type equation given in Beji (2016) and therefore is not repeated here. Retaining η_{yy} term throughout and refraining from the final spatial integration results in a generalized KP type equation for uneven depths:

$$\begin{aligned}&\left[\eta_t + C\eta_x - pCh^2\eta_{xxx} - qh^2\eta_{xxt} + \frac{3C}{4h}\left(\eta^2\right)_x + \frac{C}{4h}h_x\eta - rChh_x\eta_{xx} - shh_x\eta_{xt}\right]_x\\ &+\frac{1}{2}C\eta_{yy} = 0\end{aligned} \tag{9}$$

where the non-dimensional coefficients $p = (1+2\beta)/6$, $q = (1+\beta)/3$, $r = (15+32\beta)/24$, $s = 5(1+\beta)/6$ are employed for the sake of a simpler notation as introduced in Beji (2016). Performing the differentiation while noting that both h and C are spatially varying quantities gives another form of equation (9)

$$\begin{aligned}&\eta_{xt} + C\eta_{xx} - pCh^2\eta_{xxxx} - qh^2\eta_{xxxt} + \frac{3C}{4h}\left(\eta^2\right)_{xx}\\ &+\frac{3C}{4h}h_x\eta_x - r_pChh_x\eta_{xxx} - s_qhh_x\eta_{xxt} + \frac{1}{2}C\eta_{yy} = 0\end{aligned} \tag{10}$$

in which $r_p = r + 5p/2$ and $s_q = s + 2q$, and the second derivatives of h are neglected. The above KP type equation embodies all the known KP type equations as special cases: for constant depth setting $\beta = -1$ ($p = -1/6$, $q = 0$) gives the original KP equation while $\beta = -1/2$ ($p = 0$, $q = 1/6$) gives the KP equation corresponding to the KdV model of

Benjamin et al. (1972), the so-called BBM model. Moreover, the equation contains terms accounting for depth variations so that it can model changes in wave amplitude due to changes in water depth. Accuracy and consistency of shoaling characteristics of the unidirectional version; that is to say, the corresponding KdV equation has already been investigated analytically and shown that shoaling properties of the model equation are in exact agreement with those obtained from the constancy of energy flux (Beji, 2016). In this connection it is worthwhile to remark that Dingemans (1997) enumerates and presents derivations of various available KdV and KP type equations but none has the key shoaling terms derived above. Here, these shoaling characteristics are exploited numerically for equation (10) and their importance for reliable simulations in coastal regions with varying bathymetry is demonstrated.

2.3. Dispersion relationship of improved KP equation

Dispersion characteristics of the generalized KP type equation are now examined. Let $\eta = a_0 \exp[i(k_x x + k_y y - \omega t)]$ with a_0 denoting the constant wave amplitude, i the imaginary unit, ω the circular wave frequency, $k_x = k\cos\theta$ and $k_y = k\sin\theta$ the wave number components in the $x-$ and $y-$directions, respectively. θ is the angle wave propagation direction makes with the $x-$axis. Substituting η into the linearized, constant-depth form of equation (10) gives for ω,

$$\omega = C\left(\frac{1 + pk_x^2h^2 + \frac{1}{2}\left(k_y^2/k_x^2\right)}{1 + qk_x^2h^2}\right)k_x \tag{11}$$

where, as indicated before, $C = \sqrt{gh}$ is the non-dispersive shallow water wave celerity. Denoting $\mathbf{C}_{KP}$ as the phase velocity vector of the generalized KP type equation and recalling the relationship between the frequency and velocity $\omega = \mathbf{k}\cdot\mathbf{C}_{KP}$ with $\mathbf{k} = k_x\,\mathbf{i} + k_y\,\mathbf{j}$ for directional waves, the dispersion relationship given by equation (11) may be cast into the following form for the phase velocity vector $\mathbf{C}_{KP}$ of the new KP type equation:

$$\mathbf{C}_{KP} = C\left(\frac{1 + \frac{1}{6}(1+2\beta)k_x^2h^2 + \frac{1}{2}\left(k_y^2/k_x^2\right)}{1 + \frac{1}{3}(1+\beta)k_x^2h^2}\right)\left(\frac{k_x}{k^2}\right)\mathbf{k} \tag{12}$$

Use has been made of $p = (1+2\beta)/6$ and $q = (1+\beta)/3$ as defined before. The form of the dispersion relation corresponding to the unidirectional wave propagation in the $x-$direction is considered for selecting the optimal β value. For unidirectional waves $\theta = 0$ then $k_x = k$ and $k_y = 0$, which renders the above dispersion relationship identical with the improved or generalized KdV equation presented in Beji (2016). Without repeating the arguments and analysis presented in detail in Beji (2016) there are basically two prominent choices for β; namely, $-1/20$ or 0. If the dispersion relationship is to correspond to the fourth-order Padé approximation of the exact relationship, $\beta = -1/20$ is the choice; on the other hand, if the shoaling characteristics of the equation is to be in perfect agreement with the energy flux concept, $\beta = 0$ should be preferred. Simulations indicate negligible differences between the two choices while finite-difference scheme is in general observed to be more robust for the choice of $\beta = -1/20$ as the coefficient of η_{xxxx} becomes somewhat smaller and thus increases the stability of the scheme. Besides these two choices, different options are possible. For instance, one may prefer to improve the dispersion characteristics further hence seek a best fit to the exact dispersion curve within a preset kh range by adjusting β.

3. Numerical scheme

Finite difference schemes (Katsis and Akylas, 1987; Feng and Mitsui, 1998; Mekki and Ali, 2013) are preferable for practical applications therefore the improved KP equation is discretized by a Crank-Nicolson type implicit formulation adapted from Feng and Mitsui (1998). While the present KP equation is substantially different from the one solved by Feng and Mitsui (1998) the finite difference formulation follows their scheme closely with the exception of the treatment of η_{yy} term, which is considered here in uncoupled manner with appreciable improvement in computational efficiency.

3.1. Finite difference representation of improved KP equation

A Crank-Nicolson type discretization of equation (10) renders the following finite difference formulation.

$$\begin{aligned}
&\frac{d_x\left(\eta_{i,j}^{k+1} - \eta_{i,j}^{k}\right)}{2\Delta t\Delta x} + C_{i,j}\frac{\delta_x^2\left(\eta_{i,j}^{k+1} + \eta_{i,j}^{k}\right)}{2\Delta x^2} - pC_{i,j}h_{i,j}^2\frac{\delta_x^4\left(\eta_{i,j}^{k+1} + \eta_{i,j}^{k}\right)}{2\Delta x^4}\\
&-qh_{i,j}^2\frac{d_x\delta_x^2\left(\eta_{i,j}^{k+1} - \eta_{i,j}^{k}\right)}{2\Delta t\Delta x^3} + \frac{3C}{4h}\frac{\delta_x^2\left(f_{i,j}^{k+1} + f_{i,j}^{k}\right)}{2\Delta x^2} + \frac{3C}{4h}\frac{d_xh_{i,j}}{2\Delta x}\frac{d_x\left(\eta_{i,j}^{k+1} + \eta_{i,j}^{k}\right)}{4\Delta x}\\
&-r_pC_{i,j}h_{i,j}\frac{d_xh_{i,j}}{2\Delta x}\frac{d_x\delta_x^2\left(\eta_{i,j}^{k+1} + \eta_{i,j}^{k}\right)}{4\Delta x^3} - s_qh_{i,j}\frac{d_xh_{i,j}}{2\Delta x}\frac{\delta_x^2\left(\eta_{i,j}^{k+1} - \eta_{i,j}^{k}\right)}{\Delta t\Delta x^2} +\\
&\frac{1}{2}C_{i,j}\frac{\delta_y^2\left(\eta_{i,j}^{k+1} + \eta_{i,j}^{k}\right)}{2\Delta y^2} = 0
\end{aligned} \tag{13}$$

where the centered difference operators are defined as $d_x\eta_{i,j}^k = \eta_{i+1,j}^k - \eta_{i-1,j}^k$, $\delta_x^2\eta_{i,j}^k = \eta_{i+1,j}^k - 2\eta_{i,j}^k + \eta_{i-1,j}^k$, $d_x\delta_x^2\eta_{i,j}^k = \eta_{i+2}^k - 2\eta_{i+1,j}^k + 2\eta_{i-1,j}^k - \eta_{i-2,j}^k$, and $\delta_x^4\eta_{i,j}^k = \eta_{i+2}^k - 4\eta_{i+1,j}^k + 6\eta_{i,j}^k - 4\eta_{i-1,j}^k + \eta_{i-2,j}^k$ with i and j denoting the indices multiplying the spacings Δx and Δy between the grid points in the $x-$ and $y-$directions, respectively. $\delta_y^2\eta_{i,j}^k$ is the $y-$direction analogy of $\delta_x^2\eta_{i,j}^k$. Superscript k stands for the time level index and gives the actual time of simulation when multiplied by the time increment Δt. Note that both water depth and non-dispersive celerity are spatially varying quantities and defined at each grid point. The nonlinear function $f_{i,j}^k$ is defined as $f_{i,j}^k = \eta_{i,j}^k\eta_{i,j}^k$ and the summation $f_{i,j}^{k+1} + f_{i,j}^k$ is expressed in a semi-linear form $f_{i,j}^{k+1} + f_{i,j}^k = 2\eta_{i,j}^{k+1}\eta_{i,j}^k$ as in Feng and Mitsui (1998) for carrying out the implicit formulation without necessity of iteration due to the nonlinear term. The formal approximation procedure may be found in Feng and Mitsui (1998), the informal approach of expressing $\eta_{i,j}^{k+1}\eta_{i,j}^{k+1} + \eta_{i,j}^k\eta_{i,j}^k$ as $2\eta_{i,j}^{k+1}\eta_{i,j}^k$ may simply be attributed to the approximation that $\left(\eta_{i,j}^{k+1} - \eta_{i,j}^k\right)^2 \simeq 0$ hence $\eta_{i,j}^{k+1}\eta_{i,j}^{k+1} + \eta_{i,j}^k\eta_{i,j}^k = 2\eta_{i,j}^{k+1}\eta_{i,j}^k$.

Arranging equation (13) by placing the unknown new time level terms on the left and the known previous time level values and the complete η_{yy} discretization on the right results in a penta-diagonal matrix equation. Such a system of equations may be solved by four sweeps; the first two sweeps for reducing the system to a tri-diagonal matrix, and the next two sweeps for solving the tri-diagonal system. In this process the new time level values contained in η_{yy} on the right are treated as known in the first iteration by using only the old time level values and then introducing the new time level values in subsequent iterations. Indeed, for numerical stability this is found to be quite essential. The uncoupled treatment of η_{yy} necessarily requires iteration. During this iterative process, the semi-linearized form of the nonlinear term is avoided after the first iteration and the newly computed $\eta_{i,j}^{k+1}$ values are used in subsequent iterations in the nonlinear term without resorting to the linearization process. However, such double treatment procedure showed negligible difference when compared with semi-linearized treatment alone. Finally, only three iterations are observed to be sufficient for quite satisfying accuracy for all the cases presented here.

3.2. Treatment of boundaries

Test cases and practical applications usually require an incoming

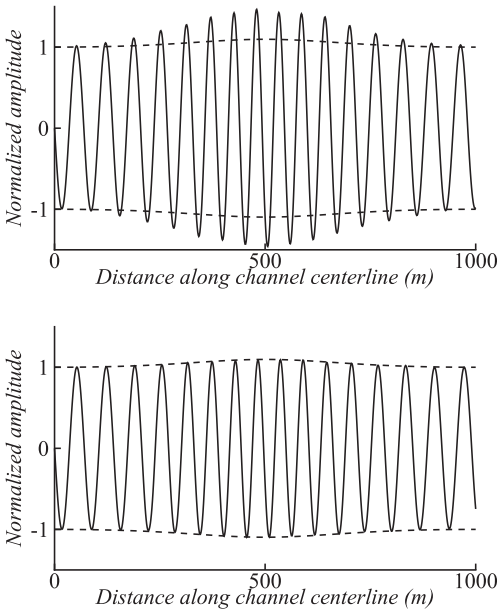

Fig. 1. Amplitude variation over a sinusoidally varying bathymetry. Envelopes (dashed lines) are computed from the constancy of energy flux. Upper graph is for BBM type KP model with only long-wave shoaling term, lower graph is for the new KP model with all the linear shoaling terms.

boundary across which incident wave field is introduced and an outgoing boundary where waves are radiated away outside the computational domain. Lateral boundaries are taken as impermeable side walls with the so-called mirror condition, $\eta_y = 0$, which is relatively simpler to implement. Introduction of incoming waves at the first node of the domain is trivial, the prescribed incident wave form is assigned numerically to the new time level surface elevation $\eta_{1,j}^{k+1}$ of the first node at each time step. Normally, the second and following nodes should be computed from the discretized wave equation. Wave equations with spatially second order derivatives result in tri-diagonal matrix systems and pose no problem in this aspect. However, in the present case the presence of both third and fourth spatial derivatives gives rise to a penta-diagonal system, as indicated before. This problem may be overcome either by one-sided discretization of these higher order derivatives or by simplifying the wave equation itself by appropriate means. One-sided discretization showed numerical instabilities and was abandoned. Instead, the unidirectional form of equation (10) in absence of $\frac{1}{2}C\eta_{yy}$ term has been simplified by the use of linear wave identity $\eta_{xx} = -k_x^2\eta$ only in the dispersion and shoaling terms so that the following equation, equation (14), has been discretized for the second, third, and the last two nodes. The last node requires a further care by backward differentiation of the second derivative.

$$\begin{aligned}&\left(1+qk_x^2h^2\right)\eta_{xt}+C\left(1+pk_x^2h^2\right)\eta_{xx}+\frac{3C}{4h}\left(\eta^2\right)_{xx}\\&+\frac{3C}{4h}h_x\eta_x+r_pCk_x^2hh_x\eta_x+s_qk_x^2hh_x\eta_t=0\end{aligned}\tag{14}$$

Frequently a radiation boundary condition is implemented on the outgoing boundary. Such a condition, being a further simplified form of the wave equation, is used simply because the wave equation itself cannot be discretized appropriately at or near the last nodal point. In this connection, use of equation (6) or its variant as proposed by Engquist and Majda (1977) may be considered as a possible choice. Ideally it should be the wave equation itself propagating the waves out without any interruption. Pursuing such an idea for Boussinesq equations and comparing the results with those obtained from the use of simple linear Sommerfeld radiation condition, Kiyokawa et al. (1996) showed the remarkable advantage of using only the wave equations in preventing artificially reflecting waves. In the present case, the simplified form of the wave equation as given by (14) with $\frac{1}{2}C\eta_{yy}$ term is deemed quite suitable.

4. Test cases

Four different tests are considered for exploring the capabilities of the newly derived KP type equation, especially over uneven depths. First, a relatively short unidirectional wave propagation over a sinusoidally varying bottom topography is simulated by the BBM type KP with only the long-wave shoaling term and by the improved KP with entire linear shoaling terms present. Both simulations are compared with the theoretical energy flux concept. Second, similar to the experimental measurements of Hammack et al. (1989), genuinely two-dimensional obliquely intersecting cnoidal waves are produced numerically by using experimentally realizable cnoidal wave parameters given in Goring and Raichlen (1980). Third, nonlinear refraction-diffraction of waves over a converging zone for three different periods are simulated and corresponding harmonic amplitudes are compared with the measurements of Whalin (1971). Finally fourth, the challenging case of wave propagation over obliquely shoaling bottom topography and obliquely situated elliptic shoal is simulated and wave height variations for definite sections are compared with the experimental measurements given in Berkhoff et al. (1982). Computations for all the test cases were carried out by performing three iterations at every time step as numerical convergence tests with four or five iterations revealed no sensible difference in results.

4.1. 1-D linear waves over bathymetry

Applications in coastal zone demand in the first place good linear shoaling characteristics as waves mainly propagate over varying water depths. Taking linear wave propagation as the zeroth-order contribution, shoaling may be accounted as a first-order effect, and inaccuracies in its estimation cannot be compensated by any other mechanism. For instance, inclusion of high order nonlinear effects would not be justifiable at all while lacking the proper mechanism of linear shoaling. Particularly for a depth-integrated wave model, for which full description of highly nonlinear wave motions is barred by the underlying theoretical framework itself, improving on nonlinearity would merely be superfluous. Furthermore, as pointed out by Stiassnie (2017) based on the work of Bonnefoy et al. (2016), weakly nonlinear theories are quite satisfactory to model nonlinearities hence inclusion of higher-order nonlinearity is not needed in practical applications. On the other hand, prediction of wave heights is an essential engineering requirement that would improve much by a reliable shoaling model. The present work thus places as much emphasis on the accuracy of linear shoaling prediction as on the accuracy of linear dispersion characteristics.

As a demonstration, linear wave propagation over a sinusoidally varying depth is simulated. Similar simulations over varying bathymetry have been reported in the relevant literature (e.g. Madsen and Sørensen, 1992; Simarro et al., 2013) for testing the linear shoaling capabilities of wave models. All these comparisons, as in here, reveal the accuracy of the proposed models for uneven depths. The water depth is initially $h_0 = 10$ m, reduces to $h_m = h_0/2 = 5$ m at mid-length of channel and then increases to $h_0 = 10$ m again. The wave period is $T = 8$ s so that at the channel entrance and exit $h_0/L_0 \simeq 1/7$ while at mid-length of channel $h_m/L_m \simeq 1/10$, both ratios indicating intermediate water waves. In Fig. 1 the upper graph shows the performance of the BBM type KP equation corresponding to $\beta = -1/2$ with only the kinematic or long-wave shoaling term $\frac{3C}{4h}h_x\eta_x$ present but the dynamic shoaling terms absent $r_p = 0$, $s_q = 0$. The lower graph shows the same simulation for the present KP equation with $\beta = -1/20$ and all the linear shoaling terms included. The wave envelope is drawn according to the energy flux concept $a^2C_g = \text{Const.}$ with C_g taken from the exact linear theory. While the BBM type KP model, which may be considered as the best available in

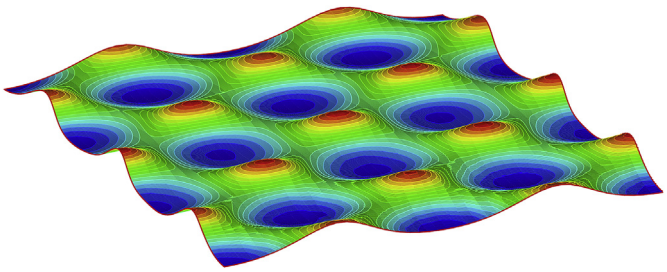

Fig. 2. A perspective view of obliquely intersecting cnoidal waves.

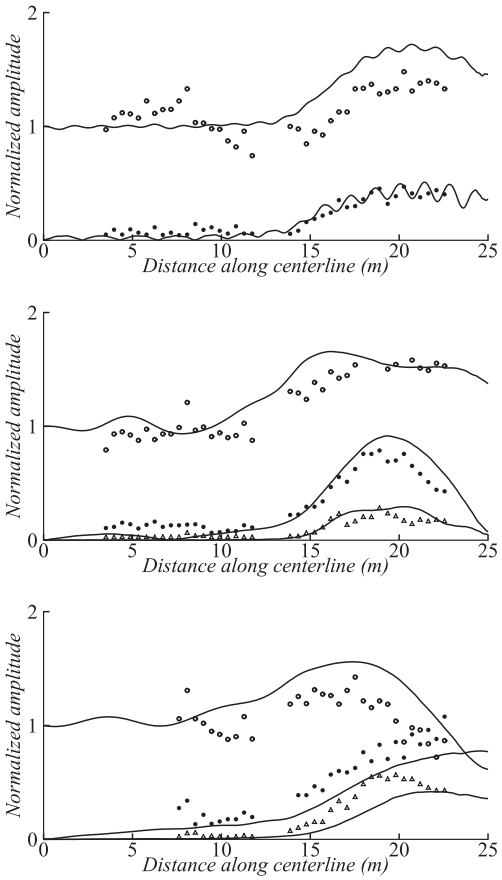

Fig. 3. Top: Whalin's experiments for incident waves of $T = 1$ s. Middle: Incident waves of $T = 2$ s. Bottom: Incident waves of $T = 3$ s. Measured and computed harmonic amplitudes along the centerline of the wave tank. Solid line: computation, scatter: experimental data.

literature, overestimates the amplitude more than 30% in mid-channel where the water depth is minimum, the present model simulation agrees with the linear theory almost perfectly.

4.2. 2-D cnoidal waves

Experiments of Goring and Raichlen (1980) revealed that physically realizable permanent cnoidal waves exist only for definite H/h, h/L and m values where H is the wave height, h the water depth, L the wavelength, and m the elliptic parameter. The wave form of $H/h = 0.05$, $h/L = 0.05$, $m = 1 - 0.215$ (CN2) from their laboratory experiments was selected for producing obliquely intersecting cnoidal waves in the manner of Hammack et al. (1989). The case is intended as a demonstration of the ability of the wave model to simulate nonlinear directional waves.

At the incident boundary along the $y-$axis two separate cnoidal wave trains directed at angles $+\theta$ and $-\theta$ to the $x-$axis were generated and superposed. Generation of a wave train with an angle to the $x-$axis was realized by introducing a time phase lag of $\Delta t_l = j\Delta y \sin\theta/c$ in the argument of the cnoidal function at each $y-$node $j = 0, \ldots, m$. This method is exactly the same as the one used by Hammack et al. (1989) in their laboratory experiments. Here, the directed wave angle was taken as $\theta = 25^o$ and the directed wavelengths in the $x-$ and $y-$directions respectively were $L_x = L/\cos\theta = 4.4$ m, $L_y = L/\sin\theta = 9.5$ m with $L = 4.0$ m being the wavelength of generating cnoidal wave. The time and spatial resolutions used were $\Delta t = T/60$ s, $\Delta x = L_x/88$ m, and $\Delta y = L_y/22$ m. The computations were done for 12 wave periods, allowing the wave field to develop fully in the entire computational domain. The length of the computational domain was taken as $15L = 60$ m and the width of the computational domain was set twice the wavelength in the $y-$direction $2L_y = 19$ m. Fig. 2 gives a perspective view for a region of $3L_x \times 2L_y$ at $t = 11.5T$.

4.3. Waves converging over topographical lens

The third case considers waves converging over a bottom topography that acts as a focusing lens (Whalin, 1971). The waves propagating over the topography converge along the mid-section of the tank and grow in amplitude, becoming nonlinear. Accordingly, higher harmonics develop and evolve with propagation distance. The experimental measurements capture these variations of the primary wave and harmonics.

The physical wave tank used in the experiments was 84 ft = 25.6 m long and 20 ft = 6.096 m wide. In the middle part of the tank eleven semicircular steps were evenly spaced to form a topographical lens. The equations describing the topography can be found in Whalin (1971). Experiments were carried out by generating regular waves with periods $T = 1, 2,$ and 3 s. Primary wave and harmonic amplitudes along the centerline of the wave tank were measured at various stations.

For all three cases the simulations were performed with a span-wise resolution Δy of $1/12$ of the wave tank width. For incident wave period $T = 1$ s, the incident wave amplitude is $a_0 = 1.95$ cm in water depth of $h_0 = 0.4572$ m. The time-step and the $x-$direction resolution were respectively $\Delta t = T/50$ s and $\Delta x = L_m/50$ m with $L_m = 1.3$ m denoting the mean wavelength computed as the average of the deep-water $h_0 = 1.5$ ft $= 0.4572$ m and shallow-water $h_s = 0.5$ ft $= 0.1524$ m wavelengths, which are $L_0 = 1.5$ m and $L_s = 1.1$ m. Note that this case is very close to deep water conditions as $h_0/L_0 = 1/3$.

Fig. 3a compares the measured data and the computed results for the primary wave and the first harmonic amplitudes for $T = 1$ s waves. In Fig. 3b the case for $T = 2$ s and $a_0 = 0.75$ cm is shown for the primary wave and two harmonics. Fig. 3c gives the same comparisons for $T = 3$ s and $a_0 = 0.68$ cm. As for $T = 1$ s case, computations for the last two cases were carried out with $\Delta t = T/50$ and $\Delta x = L_m/50$.

In this connection it is worthwhile to mention the work of Engsig-Karup et al. (2009), which is based on a fully nonlinear potential flow model. Their simulations of Whalin's (1971) experiments compare well with the data as in here while for the case of $T = 1$ s the primary wave amplitude is predicted better than the present simulation. This difference in accuracy is likely to be due to the restricted dispersive properties of the current model in deeper waters.

4.4. Waves over an elliptic shoal on a slope

Berkhoff et al. (1982) compared different wave model predictions with measurements for a rather difficult case of wave propagation over obliquely shoaling bottom topography and obliquely oriented elliptic shoal, making 20° angle with incoming wavefronts. The physical domain covered an area of 25 m × 20 m. The incident waves had the amplitude to depth ratio $a_0/h_0 = 0.05155$ and $T = 1$ s period on $h_0 = 0.45$ m water depth resulting in $h_0/L_0 = 1/3.4$, a relative depth very near Whalin's $T =$

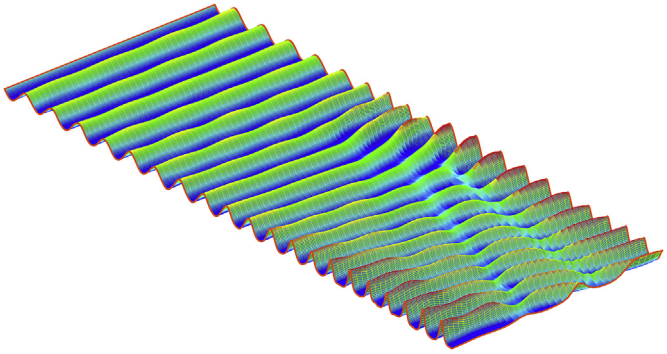

Fig. 4. A perspective view of the fully-developed numerical wave tank for experiment reported in Berkhoff et al. (1982).

1 s period case. The depth in the shallowest region over the shoal was reduced to very nearly $h_s = 0.1$ m. The results given here were produced from a computation with $\Delta t = T/60$ s, $\Delta x = L_m/60$ m, $\Delta y = W/80$ m for actual duration of 31 wave periods. Here, $L_m = 1.2$ m denotes the mean wavelength and $W = 20$ m indicates the width of the experimental basin. During the last two periods of computation the maxima and minima were determined at grid points along the measurement sections for obtaining the wave heights.

Fig. 4 shows the perspective view of the numerical wave tank after 31 periods of simulation. The converged and diverged regions of wave forms and the cnoidal character of the waves in the shallow region near the end of the domain are notable features of the simulation.

Comparisons with the experimental measurements are done for eight sections as given in Berkhoff et al. (1982). The first five sections (Section 1–5) are crosswise, taken here as the $y-$direction, while the next three sections (Section 6–8) are lengthwise along the propagation direction, the $x-$direction. Fig. 5a–e shows the transverse $y-$direction sections, zero denoting the mid-section in $x-$direction, comparing the experimental measurements with numerical simulations. Fig. 5f–h make the same comparisons for the longitudinal sections. The transverse sections are in better agreement with the measurements when compared with the longitudinal sections. This is usually true for other reported numerical models as for instance, Panchang et al. (1991) who show improved computations by using a nonlinear dispersion relationship in their essentially linear mild-slope equation model. Likewise, a numerical technique used in Engsig-Karup (2014) for fully nonlinear potential model reveals excellent agreement for all the measurement sections of Berkhoff et al. (1982). Here, the linear nature of the KP equation in the $y-$direction is likely to contribute to those observed discrepancies; however, this weakness alone may not be the only responsible element because disagreements are more prominent in the $x-$direction sections. Shortcomings associated with nonlinear dispersion characteristics of the model are too likely to play a role in these discrepancies.

5. Concluding remarks

A Kadomtsev-Petviashvili type equation for uneven water depths is derived. The new equation has improved linear dispersion and linear shoaling characteristics that extend its applicable range to virtually deep water waves. Quite challenging test cases are considered for checking the performance of the new equation against theoretical predictions and experimental measurements. In particular, linear dispersion and shoaling characteristics of the equation are quite satisfactory, allowing accurate estimation of wave heights over varying depths ranging from relatively

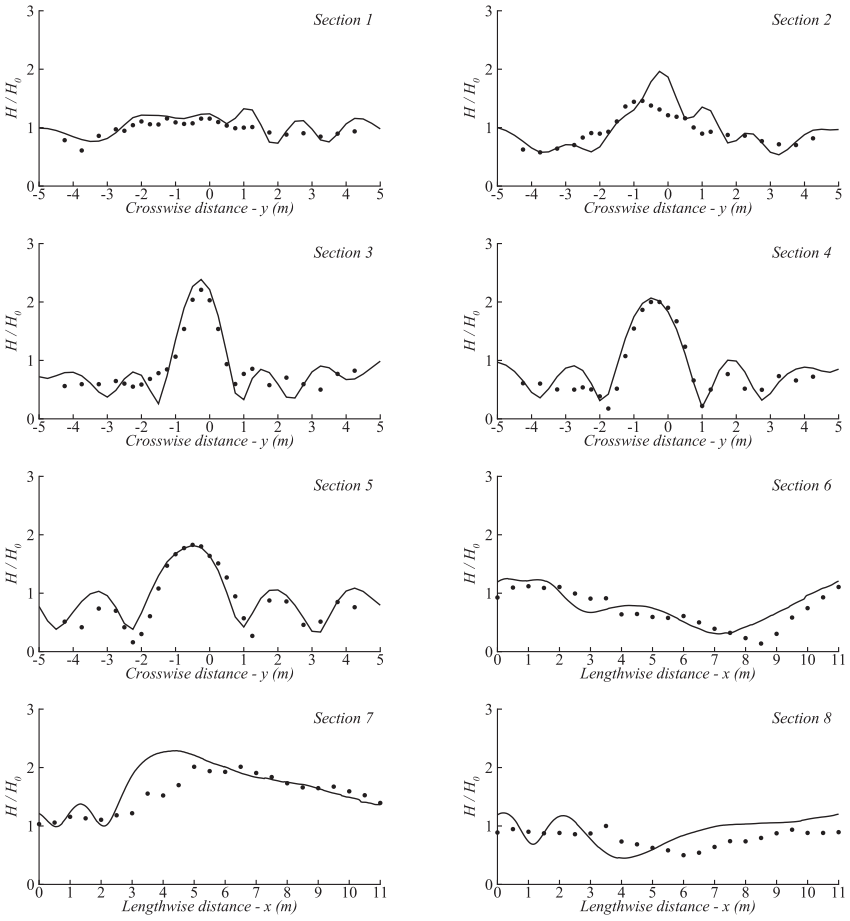

Fig. 5. Sections 1–5 are crosswise and Sections 6–8 are lengthwise comparisons of numerical simulations (solid line) with the experimental measurements (scatter) for the experiments of Berkhoff et al. (1982). Vertical scale is the normalized wave height.

deep to very shallow depths. The wave model may be used for accurate estimation of wave conditions in nearshore regions.

Appendix

The curve known as the "Witch of Agnesi" is defined in cartesian co-ordinates as

$$y = \frac{D}{(x/D)^2 + 1} \tag{.1}$$

where D is a constant denoting the diameter of generating circle. This curve was first studied by Pierre de Fermat in 1630. Guido Grandi, who gave a construction of the curve in 1703, suggested the name *versiera* from the Latin word *vertere*: to turn. Later, Maria Gaetana Agnesi (1718–1799), a remarkable woman mathematician, studied the same curve. After translation of Agnesi's book "Instituzioni Analitiche" into English the curve has become known as the "Witch of Agnesi". Supposedly, in the translation the term *versiera* used by Grandi was mistaken for the Italian word *avversiera*: witch.

Wavelike shape of the Witch of Agnesi suggests an analytical solution similar in form. After trying a more general expression of the form $A/[(x - Ct)^n + B]$, where A, B, and n are parameters to be determined and $C = \sqrt{gh}$ is the non-dispersive celerity, the following reduced form has been obtained for $B = 0$, $n = 2$.

$$\eta(x,t) = \frac{A}{(x - Ct)^2} \tag{.2}$$

Note that the form has a singularity at $x = Ct$. Singular solutions of this type for classic KdV equation have been treated in the literature (Boya, 2004; Byers and Himonas, 2004) but not for a generalized KdV equation in dimensional form as considered here

$$\eta_t + C\eta_x - pCh^2\eta_{xxx} - qh^2\eta_{xxt} + (3C/4h)\left(\eta^2\right)_x = 0 \tag{.3}$$

Substituting equation (.2) into equation (.3) results in

$$\begin{aligned} &\frac{2AC}{(x - Ct)^3} + C\frac{(-2A)}{(x - Ct)^3} - pCh^2\frac{(-24A)}{(x - Ct)^5} - qh^2\frac{(24AC)}{(x - Ct)^5} \\ &+(3C/4h)\frac{(-4A^2)}{(x - Ct)^5} = 0 \end{aligned} \tag{.4}$$

The first two terms cancel each other out; the remaining terms are gathered together as

$$\left[24ph^2 - 24qh^2 - (3A/h)\right]\frac{AC}{(x - Ct)^5} = 0 \tag{.5}$$

Terms inside the square brackets are the dispersive and nonlinear terms, which clearly show that if a permanent wave form is to be maintained they must be balanced. Equating these terms to zero requires $A = 8(p - q)h^3$. Recalling that $p = (1 + 2\beta)/6$ and $q = (1 + \beta)/3$ gives $A = -4h^3/3$, which is independent of β hence valid for any kind of KdV type equation. The final form of the solution is then

$$\eta(x,t) = -\frac{4h}{3[(x - Ct)/h]^2} \tag{.6}$$

The KP equation in its directional form does not admit any such solution in an arbitrary direction due to its unsymmetric properties with respect to $x-$ and $y-$ directions. However, the combined form of the generalized Boussinesq equation, equation (7) for constant depth, being symmetrical in both directions, does admit a solution of the form regardless of the β value:

$$\eta(x,y,t) = -\frac{4h}{3[(x\cos\theta + y\sin\theta - Ct)/h]^2} \tag{.7}$$

where θ is the angle the wave velocity vector makes with the $x-$axis.

The above solutions, though they satisfy the respective wave equations exactly, have several peculiar aspects. First, the form is always a wave of depression remaining below the free surface. Second, it travels at the non-dispersive celerity $C = \sqrt{gh}$ instead of a celerity which is a function of

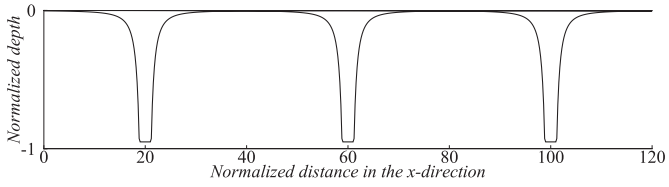

Fig. 6. Wave form according to $\eta(x,t) = -4h/3[(x - Ct)/h]^2$ for three different instances with singularities truncated at $0.95h$. Vertical and horizontal axes are normalized by the water depth h.

amplitude as is the case for nonlinear waves. Third, it is obviously singular at $x = Ct$ or $x\cos\theta + y\sin\theta = Ct$ with a trough reaching down theoretically to minus infinity or practically to bottom. Fourth, the amplitude of wave, if an amplitude can be attributed to this form, may not be selected arbitrarily and is fixed according to the water depth. Therefore, only a uniquely determined wave exists for a given depth.

Fig. 6 shows the wave form according to $\eta(x,t) = -4h/3[(x - Ct)/h]^2$. The singularities at $x = Ct$ values are truncated at $0.95h$. It is unlikely that this analytical form has any physical meaning or producibility though it does satisfy the indicated wave equation exactly. At best it could be interpreted as a mathematical peculiarity of KdV or combined Boussinesq type equations of any kind.

References

Beji, S., 2016. Improved Korteweg & de Vries type equation with consistent shoaling characteristics. Coast Eng. 109, 128–133.

Beji, S., Nadaoka, K., 1996. A formal derivation and numerical modelling of the improved Boussinesq equations for varying depth. Ocean Eng. 23 (8), 691–704.

Benjamin, T.B., Bona, J.L., Mahony, J.J., 1972. Model equations for long waves in nonlinear dispersive systems. Phil. Trans. Roy. Soc. Lond. 272, 47–78.

Berkhoff, J.C.W., Booy, N., Radder, A.C., 1982. Verification of numerical wave propagation models for simple harmonic linear water waves. Coast Eng. 6, 255–279.

Bonnefoy, F., Haudin, F., Michel, G., Semin, B., Humbert, T., Aumaître, S., Berhanu, M., Falcon, E., 2016. Observation of resonant interactions among surface gravity waves. J. Fluid Mech. 805 (R3), 1–12.

Boussinesq, J.V., 1872. Theory of waves and surges which propagate the length of a horizontal rectangular canal, imparting to the fluid contained within the canal velocities that are sensibly the same from the top to the bottom. Translated by A. C. J. Vastano and J. C. H. Mungall, March 1976 J. Math. Pure Appl. 17, 55–108.

Boya, L.J., 2004. Asymptotic irrelevance of the KdV hierarchy. Proc. Inst. Math. NAS Ukraine 50–1, 341–347.

Bryant, P.J., 1982. Two-dimensional periodic permanent waves in shallow water. J. Fluid Mech. 115, 525–532.

Byers, P., Himonas, A.A., 2004. Nonanalytical solutions of the KdV equation. Abstr. Appl. Anal. 6, 453–460.

Dingemans, M.W., 1997. Water Wave Propagation over Uneven Bottoms, Part 1-Linear Wave Propagation, Part 2-non-linear Wave Propagation. World Scientific, 967 pp.

Engquist, B., Majda, A., 1977. Absorbing boundary conditions for the numerical simulation of waves. Math. Comput. 31, 629–651.

Engsig-Karup, A.P., 2014. Analysis of efficient preconditioned defect correction methods for nonlinear water waves. Int. J. Numer. Meth. Fluid. 74 (10), 749–773.

Engsig-Karup, A.P., Bingam, H.B., Lindberg, O., 2009. An efficient flexible-order model for 3D nonlinear water waves. J. Comput. Phys. 228 (6), 2100–2118.

Feng, B.-F., Mitsui, T., 1998. A finite difference method for the Korteweg-de Vries and the Kadomtsev-Petviashvili equations. J. Comput. Appl. Math. 90, 95–116.

Goring, D., Raichlen, F., 1980. The generation of long waves in the laboratory. Proc. 17th Int. Conf. on Coastal Engineering 1, 763–783.

Hammack, J., Scheffner, N., Segur, H., 1989. Two-dimensional periodic waves in shallow water. J. Fluid Mech. 209, 567–589.

Kadomtsev, B.B., Petviashvili, V.I., 1970. On the stability of solitary waves in weakly dispersive media. Sov. Phys. Dokl. 15, 539–541.

Katsis, C., Akylas, T.R., 1987. On the excitation of long nonlinear water waves by a moving pressure distribution, Part 2, Three-dimensional effects. J. Fluid Mech. 177, 49–65.

Kiyokawa, T., Nadaoka, K., Beji, S., 1996. An open-boundary treatment for simulation of nonlinear wave propagation. Proc. Coastal Eng., JSCE 43–1, 1–5 in Japanese.

Korteweg, D.J., de Vries, G., 1895. On the change of form of long waves advancing in a rectangular canal, and on a new type of long stationary waves. Phil. Mag. 39, 422–443.

Madsen, P.A., Sørensen, O.R., 1992. A new form of the Boussinesq equations with improved linear dispersion characteristics: Part 2. A slowly-varying bathymetry. Coast Eng. 8, 183–204.

Mekki, A., Ali, M.M., 2013. Numerical simulation of Kadomtsev-Petviashvili-Benjamin-Bona-Mahony equations using finite difference method. Appl. Math. Comput. 219, 11214–11222.

Panchang, V.G., Pearce, B.R., Wei, G., Cushman-Roisin, B., 1991. Solution of the mild-slope wave problem by iteration. Appl. Ocean Res. 13–4, 187–199.

Peregrine, D.H., 1967. Long waves on a beach. J. Fluid Mech. 27–04, 815–827.

Simarro, G., Orfila, A., Galan, A., 2013. Linear shoaling in Boussinesq-type wave propagation models. Coast Eng. 80, 100–106.

Stiassnie, M., 2017. On the strength of the weakly nonlinear theory for surface gravity waves. J. Fluid Mech. 810, 1–4.

Whalin, R.W., 1971. The Limit of Applicability of Linear Wave Refraction Theory in a Convergence Zone. Res. Rep. H-71-3. U.S. Army Corps of Engrs, Waterways Expt. Station. Vicksburg, M.S.

Xue, J.-K., 2003. A spherical KP equation for dust acoustic waves. Phys. Lett. 314, 479–483.